Nuclear Science and Techniques **24** (2013) 050520

Theoretical study on fusion dynamics and evaporation residue cross sections for superheavy elements

WANG Nan[1,*] ZHAO Enguang[2,3] ZHOU Shangui[2,3]

[1]*College of Physics, Shenzhen University, Shenzhen 518060, China*

[2]*State Key Laboratory of Theoretical Physics, Institute of Theoretical Physics, Chinese Academy of Sciences, Beijing 100190, China*

[3]*Center of Theoretical Nuclear Physics, National Laboratory of Heavy Ion Accelerator, Lanzhou 730000, China*

Abstract The nuclear dynamical deformation, the fusion probability and the evaporation residue (ER) cross sections for the synthesis of superheavy nuclei are studied with the di-nuclear system model and the related dynamical potential energy surface. The intrinsic energy and the maximum dynamical deformations for ^{48}Ca+^{248}Cm are calculated. The effect of dynamical deformation on the potential energy surface and fusion is investigated. It is found that the dynamical deformation influences the potential energy surface and fusion probability significantly. The dependence of the fusion probability on the angular momentum is investigated. The ER cross sections for some superheavy nuclei in ^{48}Ca induced reactions are calculated and it is found that the theoretical results are in good agreement with the experimental results.

Key words Superheavy nuclei, Production cross section, Fusion mechanism

1 Introduction

The synthesis of superheavy nuclei (SHN) is an important and interesting field in nuclear physics. Great achievements have been obtained both in experimental and theoretical aspects. In the experimental aspect, some experiments with cold fusion reactions and hot fusion reactions[1-5] methods were carried out to synthesize the SHN with charge number up to 118. Theoretically, in order to understand the fusion process and to predict the evaporation residue cross sections, several theoretical models are put forward, such as the macroscopic dynamical model[6], the fusion-by-diffusion (FBD) models[7-12], the nuclear collectivization model[13,14], the di-nuclear system (DNS) model[15-25] and other models[26]. The evaporation residue (ER) cross sections for SHN decrease with the increase of the charge number of SHN, e.g., the ER cross section for SHN 118 is less than 1 pb. People are trying to produce the SHN with charge number larger than 118 although in former attempts no expected decay chains were observed[27,28]. Thus, it is very important to investigate the fusion dynamics and the mechanism. It is also of great necessity to give the theoretical predictions about the optimal projectile-target combination, the optimal bombarding energy and the expected ER cross sections of producing SHN because only at the optimal conditions could the SHN be successfully synthesized for their extremely low ER cross sections. If the theoretical predictions can be in good agreement with the available experimental data systematically, the model may give good predictions about the SHN which are not synthesized yet, e.g., elements 119 and 120. The heavy ion reaction is very complicated where the mass transfer is coupled with the dynamical process. Some problems in the fusion process are still unknown although much progress has been made. For example, the dynamical deformations[29-31] developed in the fusion process

Supported by National Natural Science Foundation of China (NSFC) projects (Nos.10975100, 11275098, 10979066, 11275248, 11175252 and 11120101005), MOST of China (No. 2013CB834400) and the Knowledge Innovation Project of CAS (Nos. KJCX2-EW-N01 and KJCX2-YW-N32)

* Corresponding author. *E-mail address*: wangnan@szu.edu.cn

Received date: 2013-06-27

should be taken into consideration when one investigates the heavy ion reactions. The understanding of the dynamical deformation is also important in order to calculate the ER cross sections for SHN. Thus, in this paper, the dynamical deformation in the reaction is studied and its effects on the potential energy surface and fusion probability will be investigated by using the di-nuclear system model with dynamical potential energy surface (DNS-DynPES model)[32]. The ER cross sections for some ^{48}Ca induced reactions leading to SHN with charge number 112-118 are calculated and the theoretical results are compared with the experimental results. The paper is organized as follows. In Section 2, an introduction to the theoretical model is given. In Section 3, some results about the dynamical deformation, fusion probability and evaporation residue cross sections are studied. Finally, a summary is given.

2 DNS-DynPES model

In Ref.[32], we developed a DNS-DynPES model. In this section we briefly mention the formalism for the theoretical model. Generally, the production of SHN can be separated into three stages: (1) the capture process which means the system overcoming the Coulomb barrier, (2) the fusion process which means the formation of compound nucleus (CN), (3) the de-excitation process which means the emission of neutrons to take away the excitation energy. The evaporation residue cross section in a heavy-ion fusion reaction can be written as the summation over all partial waves J as

$$\sigma_{\mathrm{ER}}(E_{\mathrm{c.m.}}) = \frac{\pi\hbar^2}{2\mu E_{\mathrm{c.m.}}}\sum_J (2J+1)T(E_{\mathrm{c.m.}},J) \cdot P_{\mathrm{CN}}(E_{\mathrm{c.m.}},J)W_{\mathrm{sur}}(E_{\mathrm{c.m.}},J) \quad (1)$$

with $E_{\mathrm{c.m.}}$ being the incident energy in the center of mass (c.m.) frame. Here $T(E_{\mathrm{c.m.}}, J)$ is the transmission probability and the survival probability $W_{\mathrm{sur}}(E_{\mathrm{c.m.}}, J)$ is calculated using a statistical model.

The DNS concept was proposed by Volkov[33] and later used to study the competition between complete fusion and quasi-fission and to calculate the fusion probability in fusion reactions[34-36].

The basic idea of the DNS model is that after the capture process, a DNS in the entrance channel is formed. Then the DNS evolves via nucleon transfer along the mass asymmetry coordinate η instead of the direction of the relative distance R between the projectile and target. If the nucleon transfer occurs from the light nucleus to the heavy one, the mass asymmetry η increases. Otherwise, if the nucleon transfer occurs from the heavy nucleus to the light one, the mass asymmetry η decreases and the quasi-fission rate increases, and that hinders the fusion. Therefore, when η is close to 1, a compound nucleus is formed with high probability, while the decrease of η away from 1, the compound nucleus formation is hindered and it may be formed with much lower probability.

We calculate the formation probability P_{CN} of a CN based on the DNS concept. During the nucleon transfer process, any configuration of DNS (A_1, A_2) with A_1 =0, 1, …., A_P + A_T and A_2 =A_P+A_T −A_1 can be formed. The evolution of the distribution function of each DNS with time can be described by a master equation

$$\frac{dP(A_1,t)}{dt} = \sum_{A_1'} W_{A_1A_1'}(t)[d_{A_1}(t)P(A_1',t) - d_{A_1'}(t)P(A_1,t)] - \Lambda_{A_1}^{\mathrm{qf}}(t)P(A_1,t). \quad (2)$$

Since A_1+A_2 =A_{P}+A_{T}, only A_1 is explicitly included in the above equation. $d_{A_1}(t)$ is the microscopic dimension for a DNS with a local excitation energy E^*_{DNS} defined in Eq.(3). E^*_{DNS} is shared by the two nuclei in this DNS.

For each nucleus, a valence space is opened due to the excitation and those nucleons in the states within the valence space are active for the transfer between the two nuclei. $d_{A_1}(t) = C_{m_1}^{N_1}\cdot C_{m_2}^{N_2}$ where N_{k} is the number of valence states and m_{k} is that of valence nucleons. $\Lambda_{A_1}^{\mathrm{qf}}(t)$ is the quasi-fission rate of the DNS(A_1, A_2) and $W_{A_1A_1'}(t) = W_{A_1'A_1}(t)$ is the mean transition probability between the DNSs(A_1, A_2) and (A_1', A_2').

In Eq.(2), the microscopic dimension, the quasi-fission rate and the mean transition probability are all related to the local excitation energy of the DNS which reads

$$E^*_{\mathrm{DNS}}(A_1,t) = E_{\mathrm{total}} - E^0_{\mathrm{DNS}}(A_1,t) - E^{\mathrm{rot}}_{\mathrm{DNS}}(A_1,t), \quad (3)$$

where

$$E_{\text{total}} = E_{\text{c.m.}} + (M_{\text{T}} + M_{\text{P}})c^2 \quad (4)$$

$$E^0_{\text{DNS}}(A_1,t) = V_{\text{DNS}}(A_1,t) + (M_1 + M_2)c^2 \quad (5)$$

$$E^{\text{rot}}_{\text{DNS}}(A_1,t) = \frac{J(J+1)}{2I_{\text{DNS}}(A_1,t)}, \quad (6)$$

$$V_{\text{DNS}}(A_1,t) = V_N(A_1,t) + V_C(A_1,t). \quad (7)$$

Here $V_{\text{N}}(A_1,t)$ is the nuclear potential calculated with a double-folding method[37] and $V_{\text{C}}(A_1,t)$ is the Coulomb interactions potential from the Wong's formula[38]. In this work a tip-tip orientation of the two deformed nuclei is assumed. The potential energy in the mass asymmetry degree of freedom (the driving potential) at t=0, is defined as

$$V_{\text{PES}}(A_1,t) \equiv V_N(A_1,t) + V_C(A_1,t) + (M_1 + M_2 - M_P - M_T)c^2. \quad (8)$$

The interaction potential between the two nuclei is related to the distance between two centers and in this paper the interaction potential takes the minimum value in the pocket.

Because of the attractive nuclear force and the repulsive Coulomb force, both nuclei in a DNS are distorted and dynamical deformations develop during the process of nuclear transfers[29-31]. This results in the time-dependence of the potential energy surface (PES). The dynamical deformations of the two nuclei satisfy $\delta\beta_1^2 C_1 / A_1 = \delta\beta_2^2 C_2 / A_2$ [13] with the stiffness parameter C_i (i=1 and 2) calculated from a liquid drop model[39]. The total dynamical deformation is the average of the dynamical deformations of the two nuclei $\delta\beta = (\delta\beta_1 + \delta\beta_2)/2$. Following Refs.[29, 31] we assume that the dynamical deformation evolves in an over-damped motion,

$$\delta\beta_t(t) = \delta\beta_{\max}(1 - e^{-t/\tau_{\text{def}}}). \quad (9)$$

In Eq.(9), the relaxation time τ_{def}=40×10^{-22} and the maximal dynamical deformation are found when the total "intrinsic" energy reaches the minimum,

$$E_{\text{int}}(A_1,\delta\beta) = V_{\text{N}}(A_1;\beta_1,\beta_2) + V_{\text{C}}(A_1;\beta_1,\beta_2) + \sum_{i=1,2}\frac{1}{2}C_i\delta\beta_i^2, \quad (10)$$

where the quadrupole deformation $\beta_i = \beta_i^0 + \delta\beta_i$ (i=1 or 2) with the static deformation parameter β_i^0 taken from Ref.[40].

3 Results and discussion

The intrinsic energy of the di-nuclear system ^{48}Ca + ^{248}Cm as a function of nuclear dynamical deformation is shown in Fig.1(a). For the configuration above, the maximum dynamical deformation for the system is about 0.32, where the minimum value for the intrinsic energy could be found and the maximum dynamical deformation is indicated as dashed line in the figure. The increase for the intrinsic energy of the di-nuclear system when β>0.32 can be attributed to the rises of the nuclear energies due to their distortions. In our calculation, it is also found that the dynamical deformations increase in the beginning 120×10^{-22} seconds and then gradually get saturated. The heavier fragment may get more significant dynamical deformation. The interaction potential for the di-nuclear system ^{48}Ca+^{248}Cm as a function of dynamical deformation is indicated in Fig.1(b) and it is found that the interaction potential decreases as increasing the dynamical deformation.

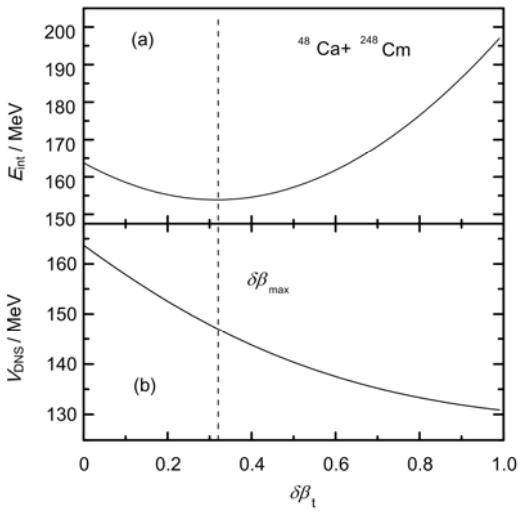

Fig.1 Intrinsic energy (a) and potential energy (b) as a function of the dynamical deformation $\delta\beta_t$ for the reaction ^{48}Ca + ^{248}Cm. The maximal dynamical deformation $\delta\beta_{\max}$ is indicated with the vertical dashed line.

The potential energy surface (the driving potential) for the reaction ^{48}Ca+^{248}Cm is shown in Fig.2. The mass and charge distributions evolve from the incident channel along the mass asymmetry degree of freedom. To form the compound nucleus, the di-nuclear configuration must overcome the highest

point on the driving potential and the barrier between the highest point and the incident channel is defined as inner fusion barrier. The solid squares in Fig.2 are for the case without dynamical deformation and the open circles are for the case when the dynamical deformation is fully developed. It is found that the potential energy surface changes significantly due to the introduction of the dynamical deformation. For example, the highest points on the driving potentials are 15.4 MeV (for solid squares) and 9.11 MeV (for open circles), respectively. The inner fusion barrier which hinders the fusion may also get influenced by dynamical deformation. The inner fusion barrier for the reaction ^{48}Ca+^{248}Cm at initial state is 18.93 MeV. While the inner fusion barrier is 29.36 MeV when the dynamical deformation is fully developed, which implies that the fusion probability may be hindered.

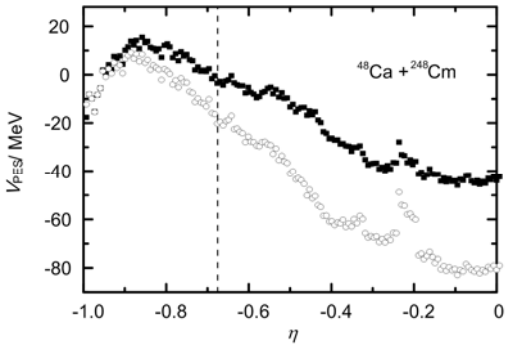

Fig.2 Potential energy surface (driving potential) for the reaction ^{48}Ca+^{248}Cm.

The fusion probability for the reaction ^{48}Ca+^{248}Cm at zero angular momentum as a function of the incident energy is depicted in Fig.3. The solid line and dashed line are for the cases with dynamical deformation and without dynamical deformation, respectively. It is found that the fusion probabilities increase with the incident energy for both the cases. When the incident energy is below 210 MeV, the fusion probabilities increase rapidly while after that the fusion probabilities increase slowly. It is also found that the fusion probability decreases significantly due to the dynamical deformation. For the case of ^{48}Ca+^{248}Cm, the fusion probability with dynamical deformation is about one order of magnitude smaller than that for the case without dynamical deformation. In Ref.[41], the fusion probability for ^{48}Ca+^{248}Cm at $E_{c.m.}$=210 MeV is found to be about 2.5×10^{-3}, which is much larger than the result in this work. Part of the difference may come from the inclusion of the dynamical deformation in this work. And it implies that more investigations about the fusion process should be carried out.

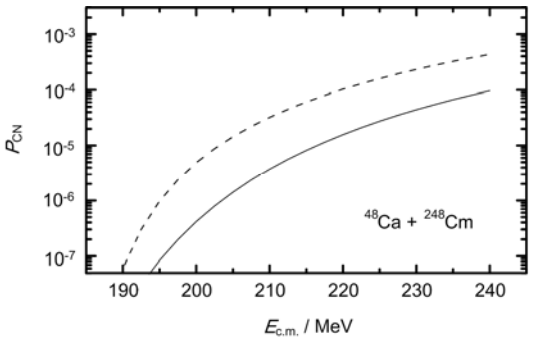

Fig.3 Fusion probabilities for the reaction ^{48}Ca + ^{248}Cm at J=0 as a function of the incident energy in c.m. frame. The solid and dashed lines are for with and without dynamical deformations, respectively.

The fusion probabilities for the reaction ^{48}Ca+^{248}Cm as a function of the angular momentum (in unit of $\hbar$) at three incident energies are depicted in Fig.4. The solid, dash dotted and dashed lines are for the cases with incident energy being 210 MeV, 200 MeV and 190 MeV, respectively. The Q value for the reaction is about −167 MeV. It is found that the fusion probability decreases as increasing the angular momentum. In the region with small angular momentum, the fusion probability decreases slowly while it drops rapidly when the angular momentum is larger than about 40 $\hbar$.

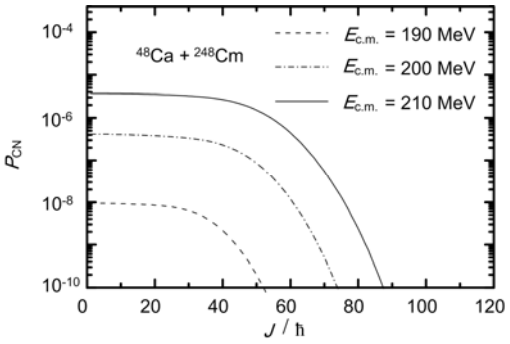

Fig.4 Fusion probabilities for the reaction ^{48}Ca+^{248}Cm as a function of the angular momentum at some incident energies.

The ER cross sections for some ^{48}Ca induced reactions leading to SHN with charge number 112−118 are calculated by using Eq.(1). The experimental optimal ER cross sections, bombarding energies and the number of the emitted neutrons[42-45]

are listed in Table 1, together with the theoretical optimal ER cross sections for the corresponding neutron emission channels. It is found that the theoretical results are in good agreement with the experimental results. After the SHN 115, the ER cross sections for the SHN appear to decrease continuously with the charge number of SHN increasing.

Table 1 Experimental optimal evaporation residue cross sections (in pb) for some reaction channels leading to SHN with Z=112−118 and the theoretical optimal results for the corresponding neutron emission channels. The incident energies in c.m. frame are in the parenthesis (in MeV).

Reactions	σ_{exp}	σ_{th}
^{48}Ca + ^{238} U	$2.45^{+1.47}_{-0.97}$ (194.7,3n)	~ 1.0 (195.0)
^{48}Ca + ^{237} Np	$0.9^{+1.6}_{-0.6}$ (202.9,3n)	~ 2.9 (202.5)
^{48}Ca + ^{242} Pu	$4.48^{+2.41}_{-1.65}$ (203.7,4n)	~ 2.4 (205.0)
^{48}Ca + ^{243} Am	$8.9^{+5.1}_{-3.9}$ (202.6,3n)	~ 3.5 (200.0)
^{48}Ca + ^{248} Cm	$3.4^{+2.7}_{-1.6}$ (208.87,4n)	~ 4.0 (207.5)
^{48}Ca + ^{249} Bk	$1.3^{+1.5}_{-0.6}$ (211.3,4n)	~ 2.5 (210.0)
^{48}Ca + ^{249} Cf	$0.5^{+1.6}_{-0.3}$ (210.4,3n)	~ 1.0 (207.5)

4 Conclusion

The nuclear dynamical deformation, the fusion probability and the evaporation residue (ER) cross sections for the synthesis of superheavy nuclei are studied using the di-nuclear system model with dynamical potential energy surface. The intrinsic energy and the maximum dynamical deformations for ^{48}Ca+^{248}Cm are investigated. The effect of the dynamical deformation on the potential energy surface is found to be significant. The fusion probability as a function of the incident energy is calculated and the dependence of the fusion probability on the angular momentum is estimated. The fusion probability is significantly hindered by the nuclear dynamical deformations. The ER cross sections for some superheavy nuclei in some ^{48}Ca induced reactions are calculated and it is found that the theoretical results are in good agreement with the experimental results.

References

1 Hofmann S and Munzenberg G. Rev Mod Phys, 2000, **72**: 733−767.

2 Morita K, Morimoto K, Kaji D, *et al*. J Phys Soc Jpn, 2004, **73**: 2593−2596.

3 Oganessian Y. J Phys G Nucl Partic, 2007, **34**: R165–R242.

4 Oganessian Y T, Abdullin F S, Bailey P D, *et al*. Phys Rev Lett, 2010, **104**: 142502.

5 Zhang Z Y, Gan Z G, Ma L, *et al*. Chin Phys Lett, 2012, **29**: 012502.

6 Bjørnholm S and Swiatecki W. Nucl Phys A, 1982, **391:** 471−504.

7 Liu Z H and Bao J D. Phys Rev C, 2009, **80:** 054608.

8 Liu Z H and Bao J D. Phys Rev C, 2011, **83:** 044613.

9 Siwek-Wilczynska K, Cap T, Wilczynski J. Int J Mod Phys E, 2010, 19: 500−507.

10 Siwek-Wilczynska K, Cap T, Kowal M, *et al*. Phys Rev C, 2012, **86:** 014611.

11 Liang Y J, Zhu M, Liu Z H, *et al*. Phys Rev C, 2012, **86:** 037602.

12 Shen C, Kosenko G and Abe Y. Phys Rev C, 2002, **66:** 061602(R).

13 Zagrebaev V I. Phys Rev C, 2001, **64:** 034606.

14 Zagrebaev V I and Greiner W. Phys Rev C, 2008, **78:** 034610.

15 Adamian G, Antonenko N, Scheid W. Nucl Phys A, 1997, **618:** 176−198;

16 Adamian G, Antonenko N, Scheid W. Phys Rev C, 2004, **69:** 011601(R).

17 Diaz-Torres A, Adamian G G, Antonenko N V, *et al.* Phys Rev C, 2001, **64:** 024604.

18 Giardina G, Hofmann S, Muminov A I, *et al.* Eur Phys J A, 2000, 8: 205−216.

19 Mandaglio G, Giardina G, Nasirov A K, *et al.* Phys Rev C, 2012, **86:** 064607.

20 Li W, Wang N, Li J F, *et al*. Europhys Lett, 2003, **64:** 750−756.

21 Li W F, Wang N, Jia F, *et al*. J Phys G Nucl Partic, 2006, **32:** 1143−1156.

22 Wang N, Li J Q, Zhao E G. Phys Rev C, 2008, **78:** 054607.

23 Wang N, Zhou S G, Zhao E G, *et al*. Chin Phys C, 2010, **34:** 1615–1621.

24 Wang N, Dou L, Zhao E G, *et al.* Chin Phys Lett, 2010, **27:** 062502.

25 Gan Z G, Zhou X H, Huang M H, *et al*. Sci China-Phys Mech Astron, 2011, **54**: s61−s66.

26 Wang N, Tian J, Scheid W. Phys Rev C, 2011, **84:** 061601(R).

27 Oganessian Y T, Utyonkov V K, Lobanov Y V. Phys Rev C, 2009, **79:** 024603.

28 Dullmann C E. “News from TASCA,” talk given at the 10th Workshop on Recoil Separator for Superheavy Element Chemistry, October 14, 2011, GSI Darmstadt, Germany.

29 Riedel C, Wolschin G, Noerenberg W. Z Phys A, 1979, **290:** 47−55.

30 Riedel C, Noerenberg W. Z Phys A, 1979, **290:** 385−391.

31 Wolschin G. Phys Lett B, 1979, **88:** 35−38.

32 Wang N, Zhao E G, Scheid W, *et al.* Phys Rev C, 2012, **85**: 041601(R).

33 Volkov V V. Phys Rep, 1978, **44**: 93−157.

34 Antonenko N V, Cherepanov E A, Nasirov A K, *et al*. Phys Lett B, 1993, **319:** 425−430.

35 Antonenko N V, Cherepanov E A, Nasirov A K, *et al*. Phys Rev C, 1995, **51:** 2635−2645.

36 Adamian G G, Antonenko N V, Scheid W, *et al.* Nucl Phys A, 1997, **627:** 361−378.

37 Adamian G G, Antonenko N V, Jolos R V, *et al*. Int J Mod Phys E, 1996, 5: 191−216.

38 Wong C Y. Phys Rev Lett, 1973, **31**: 766−769.

39 Myers W D, Swiatecki W J. Nucl Phys, 1966, **81:** 1−60.

40 Moller P, Nix J R, Myers W D, *et al*. At Data Nucl Data Tables, 1995, **59**: 185−381.

41 Nasirov A K, Kim K, Mandaglio G, *et al*. Arxiv preprint, 2013, arXiv: 1308. 1513v1.

42 Zagrebaev V I, Denikin A S, Karpov A V, *et al*. Low-energy nuclear knowledge base (Nuclear Reaction Video), [2013-9-18]. http: //nrv.jinr.ru/nrv/.

43 Oganessian Y T, Utyonkov V K, Lobanov Y V, *et al*. Phys Rev C, 2007, **76:** 011601(R).

44 OganessianY T, Utyonkov V K, Lobanov Y V. Phys Rev C, 2006, **74:** 044602.

45 OganessianY T, Abdullin F S, Bailey P D, *et al*. Phys Rev Lett, 2010, **104:** 142502.